

Environmental Impact and Aging Properties of Natural and Synthetic Transformer Oils under Electrical Stress Conditions

Peter Kurzweil,* Christian Schell, Rainer Haller,* Pavel Trnka, and Jaroslav Hornak

Against the background of environmental compatibility and unrestricted technical usability, synthetic, and natural transformer oils are critically compared in long-term tests under high voltage using electrical and instrumental analytical methods. Synthetic alkyl esters of pentaerythrol appear to be sustainable and sometimes superior substitutes for mineral oils in terms of chemical stability, viscosity, permittivity, and heat transport. Natural esters of unsaturated fatty acids are found to be unsuitable for equipment exposed to moist air. Adsorbed water appears to be a general problem in transformer oils. The aging mechanisms and molecular changes during long-term operation include radical reactions, and the formation, isomerization and cleavage of C=C bonds. Extensive material data are provided.

- 1 Mineral oil
- 2 Bio-based carbon
- 3 Synthetic ester, Figure 1^{5]}
- 4,5 Natural ester

The mineral oil-based transformer oil 1 is a mixture of paraffinic and aromatic hydrocarbons (C₁₅–C₅₀). The more biodegradable mixture 2 based on hydrocarbons from renewable sources contains almost no aromatics (see Section 2.1). The synthetic ester oil 3 is a tetraester based on pentaerythritol with linear and branched fatty acids (C₅–C₁₀) as shown in Figure 1.

In liquid-filled transformers, the oil fulfills two important functions in that it provides electrical insulation and removes the

heat generated by Joule losses mainly from the windings. The dielectric properties, such as permittivity, dissipation factor, and field strength of the electrical breakdown are important parameters when selecting oil for use in HV power transformers. As an important criterion for the insulation quality, breakdown voltage (BDV) and the partial discharge behavior (PD) of the oils are evaluated and compared in this work. The breakdown field strength, which is difficult to calculate for arbitrary geometries, is usually estimated by measuring the breakdown voltage using standardized test procedures.^[3] Some insulation quality tests are required after the transformers have been manufactured, but also during their operating time. In most cases, insulation faults are associated with partial discharges.

The heat transfer in transformer oils depends on the thermal conductivity and convection. We determined the viscosity and specific heat capacity that have the greatest impact on heat transfer.

This work examines the aging mechanisms of the oil and the solid material used to insulate the windings, which also play an important role in the selection of a suitable insulating fluid. Traces of water in the oil have a significant influence on the long-term stability of Kraft paper.^[9] A good indicator of the age of the oil is its acidity, as free carboxylic acids are released through hydrolytic cleavage and oxidation. We therefore examined the water content, the acid number and the peroxide number before and after the high-voltage tests.

1. Introduction

This work addresses the UN sustainable development goal: affordable and clean energy. As for various industrial applications of the 21st century, there is an increasing global demand for sustainable and environmentally friendly substitutes of insulating fluids used in power transformers. In high-voltage (HV) power transformers, mainly petroleum-based oils are still used, which, along with fire-safety and other environmental aspects, pose a hazard to water.^[1] Alternatives to mineral oil for use in power transformers have been sought for many years. Some promising alternatives have already been used in commercial applications.^[2–8]

With special respect to aging phenomena under thermal and electrical stress, we examined alternative insulating fluids based on natural esters and synthetic esters and compared their key properties with those of classical mineral oil.

Prof. P. Kurzweil, C. Schell
Electrochemistry Laboratory
Technical University of Applied Sciences
Kaiser-Wilhelm-Ring 23, Amberg D-92224, Germany
E-mail: p.kurzweil@oth-aw.de

Prof. R. Haller, Dr. P. Trnka, J. Hornak
Faculty of Electrical Engineering
University of West Bohemia
Univerzitní 8, Pilsen 30100, Czech Republic
E-mail: rhaller@fel.zcu.cz

 The ORCID identification number(s) for the author(s) of this article can be found under <https://doi.org/10.1002/adsu.202100079>.

© 2021 The Authors. Advanced Sustainable Systems published by Wiley-VCH GmbH. This is an open access article under the terms of the Creative Commons Attribution-NonCommercial-NoDerivs License, which permits use and distribution in any medium, provided the original work is properly cited, the use is non-commercial and no modifications or adaptations are made.

DOI: 10.1002/adsu.202100079

2. Results

2.1. Chemical Composition of Transformer Oils

In order to reveal chemical and structural changes in the molecules as a result of repeated exposure to high voltage, the oil samples were carefully analyzed before and after the long-term

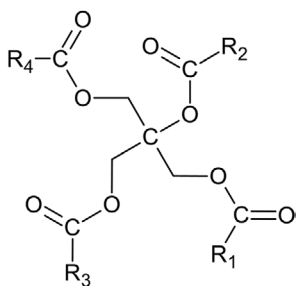


Figure 1. General formula of a synthetic ester based on pentaerythritol.

tests. For comparison, each transformer oil sample suffered at least 30 electrical breakdown events and three partial discharges (30 kV, 20 min). The tests were conducted with sinusoidal test voltage and standardized electrode arrangement (see Section 2.2).

The infrared spectra in **Figure 2** clearly differentiate between hydrocarbons (sample 1 and 2) and carboxylic acid esters (samples 3 to 5). The natural esters contain unsaturated carboxyl groups. The synthetic esters and vegetable oils were split into the underlying fatty acids with an organic base. Each sample (100 mg) *tert*-butyl methyl ether (5 mL) was transesterified with trimethyl sulfonium hydroxide (TMSH, 0.5 mL) in a headspace vial. The resulting volatile methyl esters were identified and quantified using a gas chromatography-mass spectrometry coupling (GC/MS). The separation column was nonpolar (Agilent HP-5ms, length 30 m, ID 0.25 mm, 0.25 μ m film of 5%-phenyl-methylpolysiloxane). The carrier gas was helium at a constant flow of 1 mL min⁻¹.

The synthetic ester with pentaerythritol 3 contains short-chain saturated fatty acid groups, mainly heptanoic acid to decanoic acid (**Table 1**). The fatty acids were verified with standard substances (**Figure 3**). The oil samples from different batches differ in their qualitative and quantitative composition. Interestingly, the synthetic oil contains also branched fatty acids.

The bio-based transformer oil 2 is a mixture of branched and unbranched hydrocarbons (C₁₂–C₁₈). Due to the shorter average chain length and lower molecular mass, the bio-based oil is more flammable than the classic mineral oil. The ingredients irritate the eyes, skin, and the upper respiratory tract and are slightly hazardous to water.

The natural ester products are not classified as dangerous. Sample 4 contains mainly unsaturated, unbranched fatty acids. The fatty acid pattern agrees well with that of an untreated rapeseed oil and an additional amount of oleic acid. The natural ester fluid 5 carries the fatty acid moieties of vegetable oils, mainly linoleic acid, oleic acid, palmitic acid, stearic acid, and linolenic acid. The fatty acid pattern is consistent with that of soybean oil.

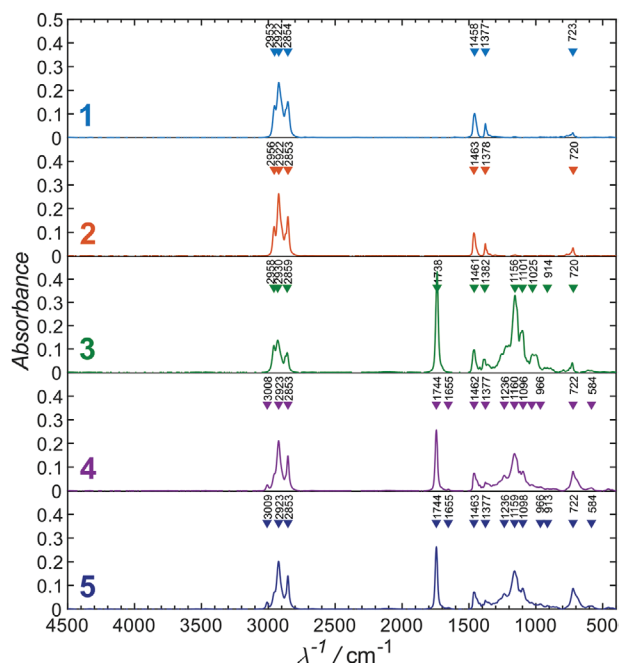


Figure 2. ATR-FTIR spectra of 1 mineral oil, 2 bio-based carbon, 3 synthetic ester, 4, 5 natural ester oils. Absorption bands: Saturated hydrocarbons at 2960, 2930, 2850, 1470, 1380, and 720 cm⁻¹. Esters around 1740, 1300, and 1000 cm⁻¹. C=C double bonds around 3010 and 1655 cm⁻¹. Numbering and details on the oils see **Table 2**.

The mineral oil 1 was analyzed directly. It consists mainly of linear and branched alkanes (C₁₂–C₃₁). Short chains play a subordinate role. Hydrocarbons are among the toxic volatile organic compounds that have a negative effect on the respiratory tract and degrease the skin. In addition, there are significant amounts of polycyclic aromatic hydrocarbons (PAHs), which explains the poor environmental impact of the oil and has a serious carcinogenic potential. The striking high sulfur content of the mineral oil lies clearly above the esters (summary see **Table 2**).

2.2. Breakdown Characteristic and Partial Discharge Behavior

As an important parameter for any design of electrical insulation, the breakdown characteristic is regularly measured using special procedures defined in relevant standards.^[10] For estimation of insulating ability as well as for comparison purposes, the breakdown voltage was measured in a special test cell at

Table 1. Fatty acid patterns (in %) of the transformer oil samples under test: *n* = linear, *iso* = branched, C=C unsaturated: mono, di, tri.

Sample	C ₇	C ₈	C ₁₀	C ₁₆	C ₁₈	Rest to 100%
3 Synthetic ester	35	10 <i>n</i> 36 <i>iso</i>	8	–	–	Short chains and C ₁₁
5 Natural ester	–	–	–	13	5 <i>n</i> 52 mono 27 di 1 tri	

Table 2. Summary of the physical-chemical parameters and chemical changes of transformer oils before and after high voltage tests [this work].

Parameter	Symbol and unit	1 Mineral oil: Nynas Nytro Taurus	2 Bio-based carbon: Nynas Nytro Bio 300x	3 Synthetic ester: Midel 7131	4 Natural ester (e.g., rapeseed): Midel eN 1204	5 Natural ester (e.g., soybean): Envirotemp FR3
Infrared bands	λ^{-1} [cm ⁻¹]					
$\nu(\text{CH}_2, \text{CH}_3)$ above 3000 cm ⁻¹		–	–	–	Weak	Weak
$\nu(\text{CH}_2, \text{CH}_3)$ below 3000 cm ⁻¹		3 Strong bands	3 Strong bands	3 Strong bands	2 + shoulder	2 + shoulder
$\nu(\text{C}=\text{O})$ around 1740 cm ⁻¹		–	–	Strong	Strong	Strong
$\nu(\text{CH})$ around 1460 and 1380 cm ⁻¹		Medium	Medium	Medium	Medium	Medium
$\nu(\text{C}-\text{O})$ at 1240, 1160, 1100 cm ⁻¹		–	–	Medium	Medium	Medium
$\delta(\text{CH})$ at 720 cm ⁻¹		Very weak	Weak	Weak	Medium	Medium
Additional weak bands		–	–	1025, 914	966, 585	966, 913, 585
Alkyl rests						
– Short chain		Yes	–	C ₇ to C ₁₀	–	–
– Long chain: linear and branched		C ₁₂ to C ₃₁	C ₁₂ to C ₁₈	–	C ₁₆ to C ₂₂	C ₁₄ to C ₂₂
– PAH		Yes	–	–	–	–
– Unsaturated C=C		–	–	–	Yes	Yes
Changes after high-voltage tests		More CH ₂ , C=O; less CH ₃	Not significant, less CH ₃	Not significant, more H ₂ O, C=O	More C=C	More <i>trans</i> -C=C, less BHT
Water content	$w(\text{H}_2\text{O})$ [mg kg ⁻¹]					
Dried and after storage		1.5 ... 6.5	3.8 ... 16	2.6 ... 14	25 ... 99	32
Saturation value in 100% r.h.		44	44	1250	850	870
After BDF/PD experiment		14	27	355	–	281
Total acid number (TAN)	$w(\text{KOH})$ [g kg ⁻¹]					
New sample		0.007	0.03	0.11	0.12	0.12
After high-voltage test		0.009	–	0.19	–	0.18
Saponification number	$w(\text{KOH})$ [g kg ⁻¹]					
New sample		0	0	274	176	170
After high-voltage test		–	–	185	–	184
Iodine number	$w(\text{I}_2)$ [g kg ⁻¹]					
New sample		19	16	11	1188	1330
After high-voltage test		26	2	1	–	1360
Peroxide number	$w(\text{O}_2)$ [mmol kg ⁻¹]					
New sample		–	0.02	0.034	0.077	0.094
After high-voltage test		–	–	0.10	–	83000
Density (20 °C)	ρ [g cm ⁻³]	0.859	0.782	0.967	0.916	0.920
Linear decrease 20... 100 °C	$\Delta\rho/\Delta T$ in g cm ⁻³ K ⁻¹	–0.000 65	–0.000 067	–0.000 071	–0.000 065	–0.000 075
Viscosity (40 °C)	η [mPa s]	8.42	2.87	28.2	33.3	31.2
Decrease 20 ... 100 °C		medium: 18 ...2.3	low: 5.0 ... 1.1	high: 68 ... 5.8	high: 76 ... 7.7	high: 68 ... 7.2
Kinematic viscosity (40 °C)	ν [mm ² s ⁻¹]	9.95	3.72	29.5	36.9	34.5
Specific heat capacity (40 °C)	c_p [J kg ⁻¹ K ⁻¹]	1930	2110	1896	2014	1924
Linear increase –20→ 120 °C		1700... 2240	1900... 2400	1750... 2120	1900... 2250	1860... 2150
Crystallization temperature	T_c [°C]	<–40	–35.5	<–40	–20.2	–13
Latent heat (exotherm)	ΔH [kJ kg ⁻¹]	–	0.38	–	0.26	1.0
Permittivity (50 Hz, 40 °C)	ϵ_r	2.03	1.90	2.89	2.85	2.86
Range between 20 and 80 °C		2.04 ... 1.96	1.92 ... 1.86	2.92 ... 2.71	2.90 ... 2.69	2.91 ... 2.71
Dissipation factor (50 Hz, 40 °C)	$\tan \delta$	0.0009	0.0004	0.0047	0.0019	0.0012
Increase between 20 and 90 °C		Small: << 0.01	Small: << 0.01	High: up to 0.05	Medium: < 0.03	Medium: < 0.02
Evaporation temperature	T_z [°C]	>100	>120	>250	>350	>350
Decomposition temperature		174	169	309	386	380
Decomposition products under nitrogen atmosphere		Broken chains, alkanes	Alkanes, acids, ketenes	Alkanes, methyl esters	Ester cleavage, C=C aldehydes	Ester cleavage, C=C aldehydes

Table 2. Continued.

Parameter	Symbol and unit	1 Mineral oil: Nynas Nytro Taurus	2 Bio-based carbon: Nynas Nytro Bio 300x	3 Synthetic ester: Midel 7131	4 Natural ester (e.g., rapeseed): Midel eN 1204	5 Natural ester (e.g., soybean): Envirotemp FR3
Elemental analysis	β [$\mu\text{g L}^{-1}$]					
Na		96	168	390	11	6
Ca (traces: Sr, Ba)		43	1	–	–	–
Cr		6	9	(1)	50	5
Fe		–	18	2	–	–
Ni		5	23	–	–	–
Cu		3	5	3	4	3
Zn		16	38	6	24	13
Hg		5	2	26	1	1
B		174	324	–	128	31
Al		46	116	443	28	28
Pb		–	–	133	–	1
As		3	1	1	–	–
Se (traces: Te)		1 (1)	–	–	–	–
Sulfur		187	5.4	4.9	4.9	18.6

AC stress voltage under defined conditions. The test electrode system is designed in such a way that it forms a more or less uniform electrical field, while the test voltage is increased until the ionization process within the liquid begins and a breakdown is initiated. The measured value of the breakdown voltage is obtained by repeated tests due to the stochastic character of breakdown process.

As shown in Figure 4, the bio-based carbon oil provides the highest value of the breakdown voltage: 62 kV is about 30% above the lowest value measured at natural ester fluids.

For comparison and design purposes, however, the electric breakdown field strength E_{bd} is commonly used, which is given by the breakdown voltage U_{bd} and the electrode gap $s = 2.5$ mm of the test system in Equation (1)^[11]

$$E_{bd} = \frac{U_{bd}}{s \eta} \quad (1)$$

The field efficiency factor of the test system was $\eta = 0.98$ which provides a quasiuniform electrical field (Figure 4a). As

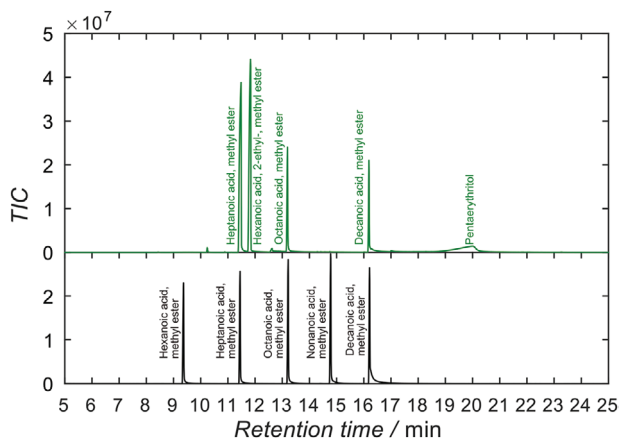
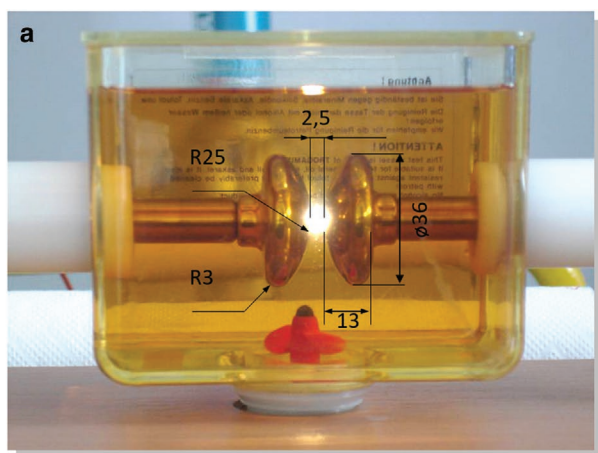


Figure 3. GC-MS analysis of the synthetic ester oil 3 (green) compared with a standard mixture of linear fatty acid methyl esters (C_7 – C_{11}).

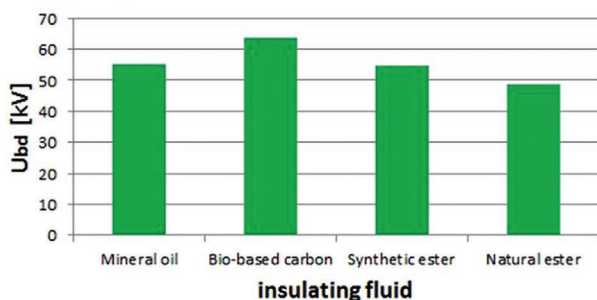
expected the breakdown field strength values follow the same tendency as the voltage. For the bio-based carbon oil, about 26 kV mm^{-1} was measured.

In accordance with standardized requirements, the breakdown tests were carried out under quasiuniform electrical field conditions. That means, before a breakdown occurs, no PD behavior can be investigated, since any discharge activity immediately leads to the breakdown. Therefore, for studying partial discharge, a test arrangement with nonuniform electric field was designed (Figure 5a, $s = 10$ mm, $\eta \approx 0.1$). With such an arrangement, the PD process begins when the field strength is high enough to initiate discharges. This level is characterized by the inception voltage (PDIV). If the test voltage exceeds the PDIV value and after it has fallen below a certain value again, the partial discharge process is stopped at the extinction voltage (PDEV). Both voltage parameters characterize every PD behavior of the electrical insulation. In addition to these values, the partial discharge is described by the measured electric charge Q , which is proportionally to the PD intensity and is therefore well appropriate for any comparison purposes. For the liquids examined, the inception and extinction voltages in Figure 5 show that the PD activity in the bio-based carbon fluid is initiated at a lower voltage and electrical field strength than with the other oils. Taking into account the high breakdown values, the PD activity does not lead to any higher harmful breakdown condition, even at high test voltages of 30 kV. And the PD intensity is also relatively low. A similar behavior can be observed for mineral oil with some higher PDIV/PDEV values.

Completely different results were obtained with the ester fluids. The extinction voltage (PDEV) is always significantly lower than the inception voltage (PDIV). This could indicate a certain capability of “charge storage” within the fluid (hysteresis), which could lead to a harmful effect on the electrical breakdown. The above results are confirmed in principle by the dependence of the electric charge on the stress time, in that the test voltage was continuously increased after reaching PDIV. Figure 6 shows that in the case of ester fluids, the breakdown occurs after 200 or 400 s at relatively high charge levels.



b electric breakdown voltage vs fluid type



c electric breakdown field strength vs fluid type

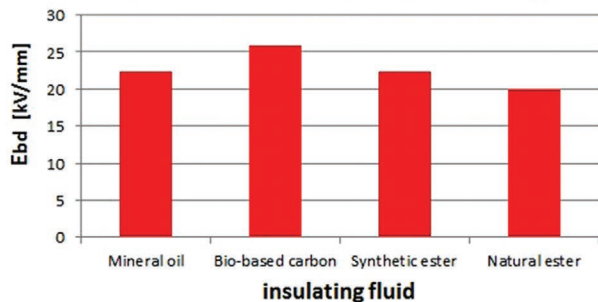


Figure 4. a) Practical test cell with 2.5 mm electrode distance according to IEC 60 156. The sinusoidal test voltage is increased with $\approx 1 \text{ kV s}^{-1}$ up to breakdown, until at least 6 and a maximum of 20 repeated breakdowns are achieved. b) Breakdown voltage and c) breakdown field strength of different transformer fluids.

2.3. Permittivity and Dissipation Factor

The dielectric behavior of the transformer oils was investigated by the help of impedance spectroscopy using a SOLATRON SI 1260 frequency-response analyzer. The permittivity of each sample was determined relatively to the empty test cell filled with air in a drying cabinet at various temperatures. The relative permittivity ϵ_r results from the capacitance $C(\omega)$

$$\epsilon_r = \frac{C_{\text{oil}}}{C_{\text{air}}} = \frac{\epsilon_r \cdot \epsilon_0 \cdot A/d}{\epsilon_0 \cdot A/d} \quad \text{and} \quad C(\omega) = \frac{-\text{Im} Z}{\omega |Z|^2} \quad (2)$$

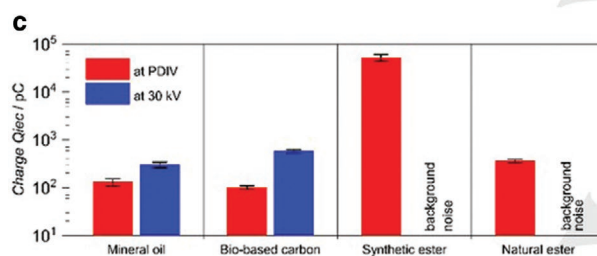
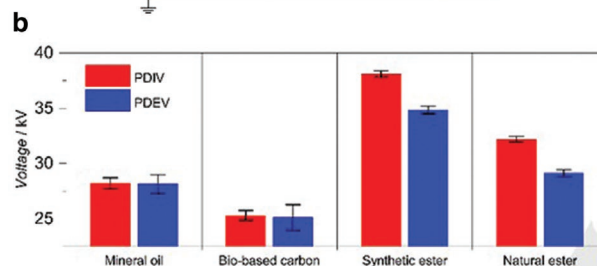
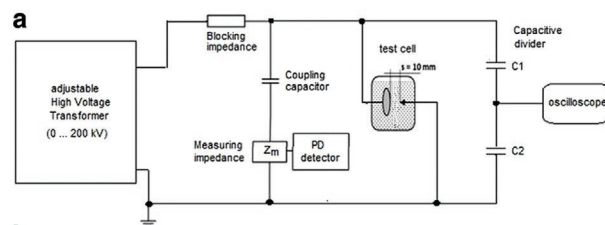


Figure 5. Partial discharge behavior of different transformer fluids: a) test circuit (IEC 111), b) inception and extinction voltage, and c) electric charge.

For a RC series combination, the loss factor equals

$$\tan \delta(\omega) = \omega \cdot C(\omega) \cdot R(\omega) \quad (3)$$

wherein $\omega = 2\pi f$ is the angular frequency and $R(\omega)$ is the equivalent series resistance. A is the electrode area, and d is the electrode distance.

The synthetic and natural ester oils exhibit an ≈ 1.5 times higher permittivity compared to the hydrocarbon-based oils (Figure 7). The dissipation factor rises exponentially with

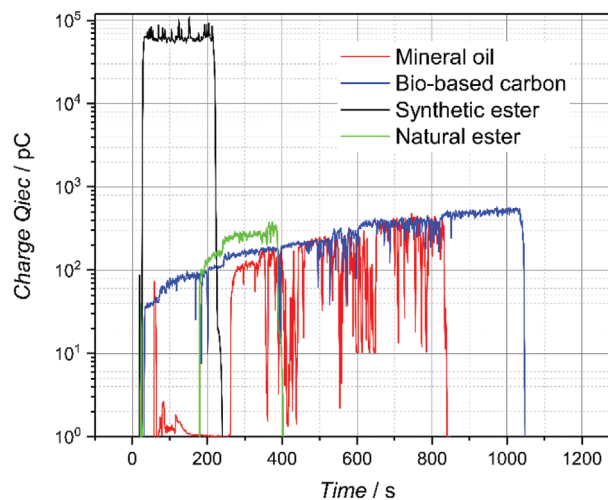


Figure 6. Electric charge versus stress time at increasing test voltage.

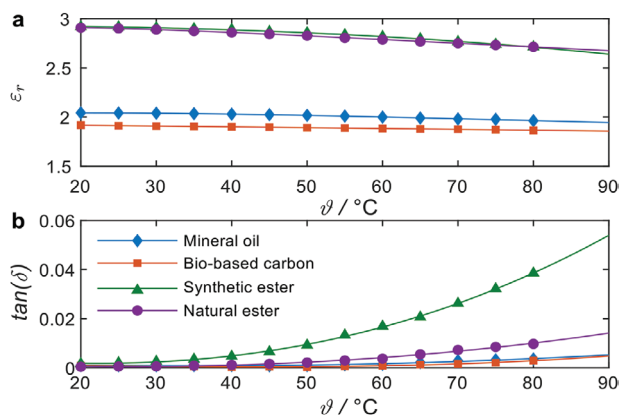


Figure 7. Permittivity a) and dissipation factor b) at 50 Hz.

increasing temperature. Obviously, the number and mobility of the charge carriers are increased by thermal dissociation and improved viscosity, which is typical for an ionic conduction mechanism.^[12]

On the other hand, the hydrocarbon-based oils have a significant lower dissipation factor. No significant changes in permittivity and dissipation factor were found after the high-voltage tests (see Section 2.2). Within the measurement error, the high-voltage tests did not significantly increase the conductivity of the oils (below $0.01 \mu\text{S cm}^{-1}$). See Section 3.

2.4. Cooling Properties of the Oils

The density was determined according to the Archimedes' principle using a buoyancy body in a thermostatically controlled vessel. There is an excellent linear correlation between density and temperature, $\rho(\vartheta) = \rho(20 \text{ }^\circ\text{C}) + \text{const} \cdot \vartheta$, as shown in Figure 8. The bio-based carbon oil has the lowest density 78 g cm^{-3} , the synthetic ester has the highest density (0.97 g cm^{-3}), The density of the natural esters lies in between (0.92 g cm^{-3}).

The temperature-dependent viscosity was measured using a Höppler falling ball viscometer at defined temperatures between $\vartheta = 20$ and $90 \text{ }^\circ\text{C}$. The measured values were fitted

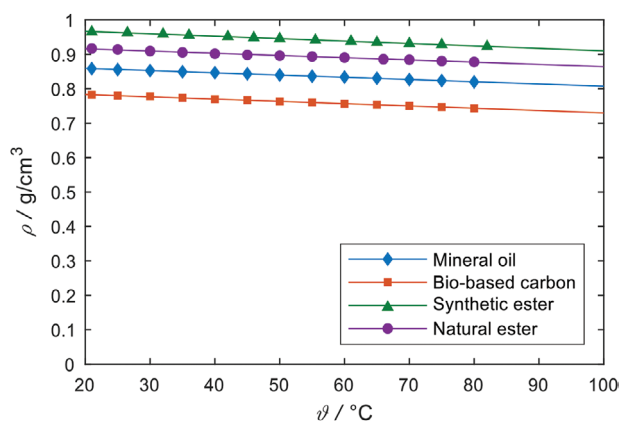


Figure 8. Temperature-dependent density.

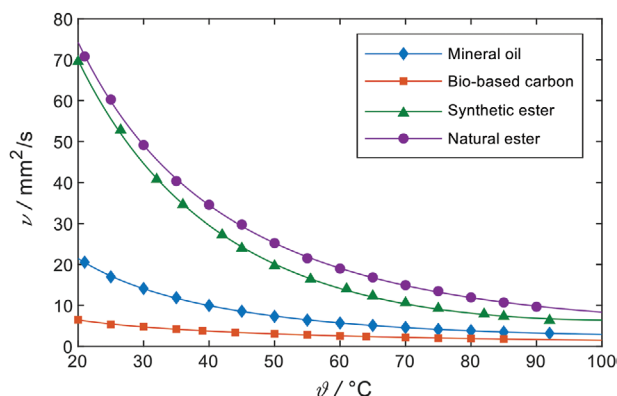


Figure 9. Temperature-dependent kinematic viscosity.

and extrapolated according to Equation (4) which provides high accuracy and extrapolation security^[13]

$$\nu(\vartheta) = E \cdot \exp \left[A \left(\frac{C - \vartheta}{\vartheta - D} \right)^{1/3} + B \left(\frac{C - \vartheta}{\vartheta - D} \right)^{4/3} \right] \quad (4)$$

For the case that the term $(C - \vartheta)/(\vartheta - D)$ becomes negative, the correct relationship reads

$$\begin{aligned} \left(\frac{C - \vartheta}{\vartheta - D} \right)^{1/3} &= - \left(\frac{\vartheta - C}{\vartheta - D} \right)^{1/3} \\ \left(\frac{C - \vartheta}{\vartheta - D} \right)^{4/3} &= - \left(\frac{\vartheta - C}{\vartheta - D} \right)^{1/3} \left(\frac{C - \vartheta}{\vartheta - D} \right) \end{aligned} \quad (5)$$

Especially in the lower temperature range, the viscosity of the ester oils is considerably higher than that of the hydrocarbon-based liquids (Figure 9). The higher viscosity has a great influence on the cooling properties of the oil and the oil circulation in the transformer. The heat transport from the windings in ester oils is worse compared to mineral oil. However, in the upper temperature range, where the cooling properties become more important, the differences between ester oils and mineral oil are no longer so great. Nevertheless, the differences in viscosity must be considered when designing the transformer.

The specific heat capacity, which also affects the cooling properties of the oil, was determined using the so-called sapphire method of differential scanning calorimetry. At first, an empty crucible determines all deviations from the theoretical zero line, which are caused by asymmetrical masses, placements, and device-specific features. Then the sapphire standard with known temperature dependent c_p values is measured. Finally, each oil sample was examined in triplicate. The specific heat capacity in Equation (6) is given by the masses m and heat flow Φ through the oil, the sapphire crystal (s) and the empty crucible (c)

$$c_p = \frac{\Phi - \Phi_c}{m} \cdot \frac{m_s}{\Phi_s - \Phi_c} \cdot c_{p,s} \quad (6)$$

The c_p values of the insulating fluids are comparable. The slope $dc_p/d\vartheta$ of the hydrocarbon-based oils is greater than that of the ester oils (Figure 10). However, the natural esters exhibit a phase transition, the crystallization, at around $-20 \text{ }^\circ\text{C}$.

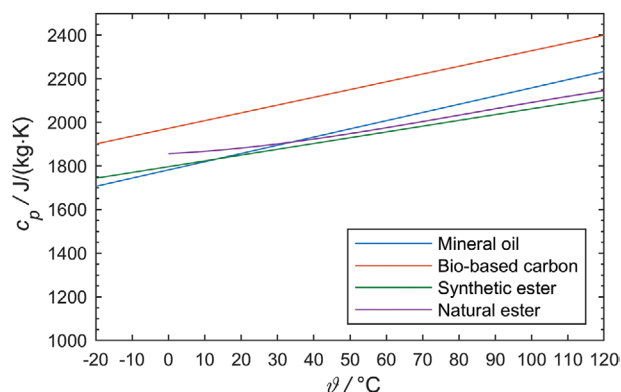


Figure 10. Temperature-dependent specific heat capacity.

The high voltage test (Section 2.3) had no adverse effect on the viscosity, although it has been reported that the viscosity can increase significantly due to thermal aging.^[3]

2.5. Water Content and Relative Humidity

The water content of the oils was determined by coulometric Karl Fischer titration, which determines both the physically dissolved water and the associated water. The oil samples were compared in dry and saturated condition before and after the high voltage tests.

With increasing ambient humidity, the transformer oils accumulate water and the breakdown voltage decreases. The relative humidity of the oil is defined by the ratio of the absolute amount of water to the saturation amount of water at the same temperature, $\phi = m/m_s$. Despite the relatively high saturation level of water in the synthetic and natural esters, the relative humidity in new samples is lower than 4% (Figure 11).

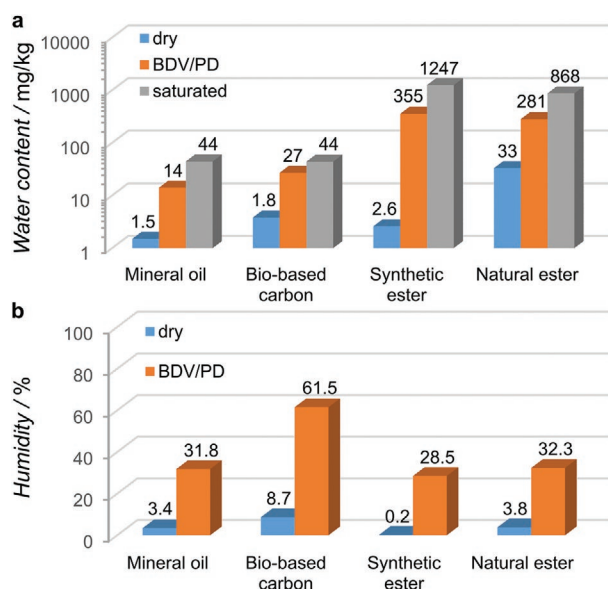


Figure 11. a) Absolute water content of the transformer oils in dry and saturated condition and after the high voltage tests. b) Relative humidity.

Mineral oil and bio-based carbon physically dissolve water, while the ester liquids are able to take up traces of water also in chemical bonds and hydrogen bridges. Hydration effects influence the mobility of ions and thus increase the permittivity of the moist oil compared with the dry fluid. The ester oil can advantageously absorb water from the Kraft paper and thereby prevent the cellulose from polymerizing.

The absolute water content of the ester oils increases significantly during the high-voltage tests, i.e., water is absorbed from the ambient or is generated by chemical reactions. The water content of mineral oil and bio-based carbon grows less badly.

2.6. Decomposition Products in Technical Use

An advantage of vegetable oil over mineral oil is the higher flash point.^[3,5,13,14] The hydrocarbon-based oils decompose above 150 °C, while the synthetic and natural esters are stable up to 300 °C. The thermogravimetric analyses under nitrogen atmosphere are compiled in Figure 12 and Table 2. By heating, the mineral oil liberates alkanes, alcohols, and carboxylic acids. The synthetic ester decomposes in alkanes and methyl esters. The natural esters form saturated and unsaturated hydrocarbons and aldehydes, methyl esters, and CO₂.

The crystallization temperature (pour point) was determined by differential scanning calorimetry. The oil samples were cooled down to -40 °C with a cooling rate of 1 K min⁻¹ and the differential heat flow was evaluated (Figure 13). The natural ester and the bio-based mineral oil exhibit phase changes by crystallization below -10 °C. Such a pour point is determined by the high hydrocarbon content.

The total acid number (TAN)^[15] obtained from the titration curves is slightly higher with the ester fluids compared to the hydrocarbon-based oils (Figure 14). Each oil sample (20 g) was dissolved in an ethanol-diethyl ether mixture (1 : 1, 50 mL) and treated with potassium hydroxide solution (0.01 mol L⁻¹). Significantly, the natural ester shows an increase in acidity after breakdown voltage and partial discharge tests. This means that acid molecule fragments are formed by electrical breakdown.

The peroxide value is a measure of the undesired oxidation of fats and oils. Each oil sample (5 g) was dissolved in a mixture of acetic acid and chloroform, containing additional saturated potassium iodide solution (0.5 mL). Excreted iodine is titrated with sodium thiosulfate solution (0.1 mol L⁻¹) against a starch indicator. In accordance to the TAN, the peroxide value of the natural ester shows a strong increase after the high voltage tests.

3. Discussion

3.1. Chemical Stability and Aging Phenomena

At first glance it is somewhat surprising that oils with a large amount of unsaturated fatty acids should be used as insulating liquids in transformers. The C=C double bonds can basically react with traces of water and oxygen. Significantly, natural esters form free fatty acids, peroxides, and unsaturated compounds. Under thermal stress, vegetable oils age by hydrolytic

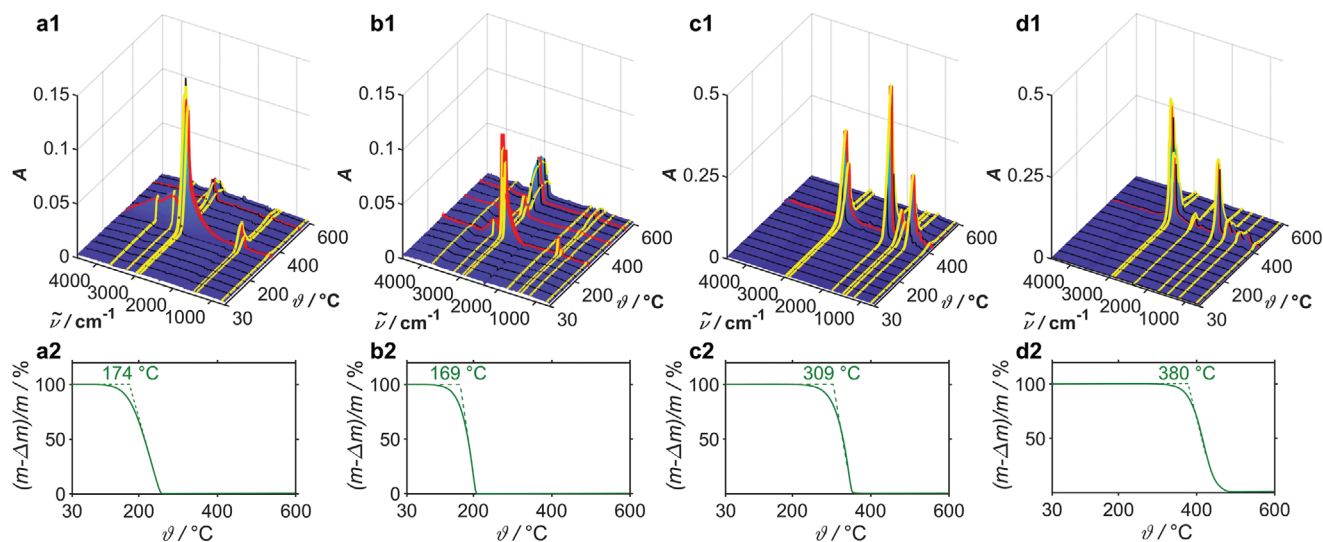
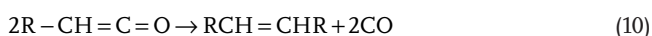
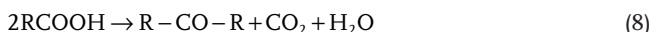
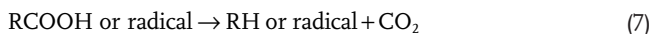


Figure 12. TGA-IR measurements using a NETSCH TG 209 F1 Libra device coupled with a BRUKER TENSOR 27 IR spectrometer: a mineral oil, b bio-based carbon, c synthetic ester, d natural ester: 1 = nitrogen atmosphere in a closed crucible, 2 = under nitrogen in an open crucible. Heating rate 5 K min⁻¹.

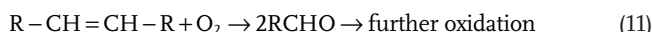
scission, oxidation, and polymerization. Our analyses confirm known decomposition reactions^[16–21] of fatty acids, which produce alkanes, CO₂ and ketones when heated. Generally, natural ester oils create more gases, including hydrogen and ethane, under thermal stress than synthetic esters and mineral oil. Triglycerides are partly split in reactive ketenes that are the origin of toxic acrolein and unsaturated compounds



Hydroperoxides are primarily generated as the first oxidation compound from which all secondary decomposition

products are derived: 1) fatty acids by hydrolysis and elimination of hydrogen. 2) Polymerization creates ketones and other high molecular weight compounds that increase viscosity. Volatile aldehydes are responsible for rancid odors. 3) Nonvolatile epoxides are formed from volatile compounds.

Unsaturated fatty acids are split into aldehydes. Aging under the presence of air causes increasing viscosity with the natural esters, because the fatty acid radicals form polymer chains^[3]



During thermal and electrical breakdown aging, mineral oils change from colorless to yellow-brown. Vegetable oils in particular form C=C double bonds under constant electric stress (Figure 15). The increased optical absorption^[22] around 300 nm might indicate the formation of unsaturated carbonyl compounds and polymers thereof.

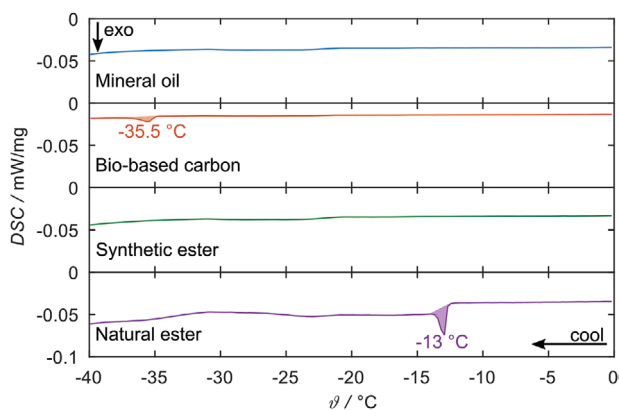


Figure 13. DSC measurements using a “NETZSCH DSC 214 Polyma” device: crystallization at a cooling rate of 1 K min⁻¹.

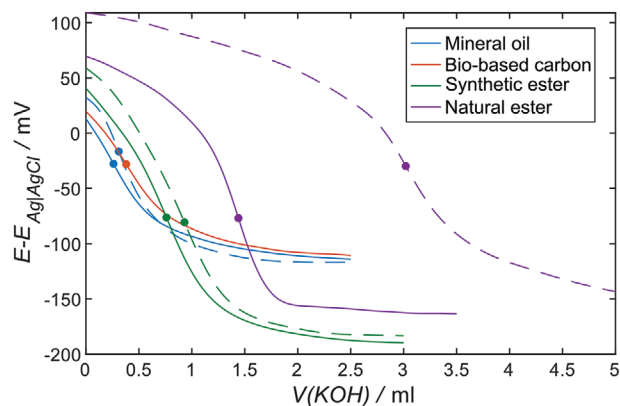


Figure 14. Controlled-current potentiometric titration of the oil samples with 0.01 molar KOH solution. Schott Titroline alpha, IrO₂ electrode versus Ag|AgCl. Solid lines: new oils. Dashed: after the high voltage tests.

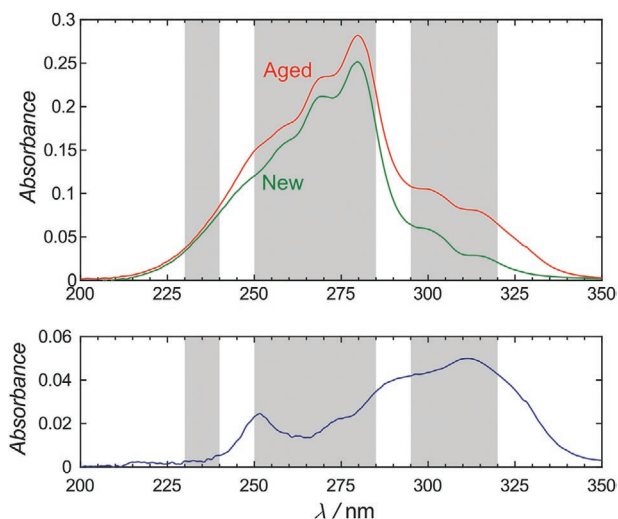


Figure 15. UV-vis spectrum of the natural ester 5 before and after the high voltage tests. Below: Spectral difference.

In the long-term test under electrical breakdown, partial discharge with paper barrier, or high temperature, chemical bonds are split. Multivalent alcohols are formed in the mineral oil very slowly. The total acid number increases slightly during aging, because free acids are generated in all samples. As well, the synthetic ester is split. However, the negligible amount of free fatty acids does not cause any unwanted pH changes that could be harmful to the paper insulation. With respect to the critical depolymerization of the paper separator, mineral oil appears to be the most aggressive medium.^[3]

The water problem—Basically, the synthetic and natural ester oils solve more water than mineral oil ($\gg 100 \text{ mg kg}^{-1}$). This can be explained in terms of the hydrogen bonds between polar OH-groups and surrounding water molecules. Aging increases the water content in all samples. In the vegetable oils, hydrophilic decomposition products attract additional water molecules. It is known that the AC breakdown voltage of natural esters is determined by hydrogen bridges and traces of water.^[23,24] Water in humidified samples accelerates the degradation rate of oil-paper insulation system by hydrolysis processes and acids products.^[25,26]

The peroxide value appears to be a good parameter for monitoring the aging behavior. The initial oxidation products that accumulate in ester oils are hydroperoxides, which subsequently form lower-molecular alcohols, aldehydes, free fatty acids, and ketones, leading to autooxidative rancidity. The greater aging of the natural ester can be explained by the unsaturated fatty acids contained in the oil. The C=C double bonds are less stable to oxidation than saturated C—C bonds. Therefore, the natural ester oils should only be used in airtight transformers, to minimize contact with oxygen.

These results are semiquantitative as the total number of electrical breakdowns and partial discharges was not exactly the same for all oils. However, it becomes clear that the unsaturated vegetable oils age faster than the synthetic esters in the electric field due to oxidation and radical reactions.

3.2. Electrical and Thermomechanical Properties

The ester oils exhibit greater permittivity ($\epsilon_r \approx 2.8$) than the mineral oil ($\epsilon_r \approx 2$), which however is less dependent on temperature and shows the lower dissipation factor ($\tan \delta < 0.01$). The weak electrical conductivity of all transformer oils is caused by less than 1 mg kg^{-1} of dissolved ions (Na^+ , Zn^{2+} , B species, Al^{3+}). During aging, the dissipation factor increases in all oil samples.

The breakdown voltage and insulation strength of the ester oils is very good even in moist and aged samples—and better than with mineral oil. Obviously chemical changes during aging do not affect the quality of vegetable oils for power transformer applications. Mineral oil suffers a dramatic loss of dielectric strength. However, the higher generation of electrostatic charges at the paper/vegetable oil interface must be further investigated with respect to partial discharges and breakdown of the transformer.

The thermal stability is coined by phase transitions between -20 and 0 °C. Thanks to the mixture of esters, vegetable oils do not suddenly freeze or thaw, and remain in a liquid state even at very low outside temperatures.

The ester oils exhibit higher decomposition temperatures (≥ 300 °C) than the mineral oil (≈ 170 °C). The more stable specific heat capacity of the ester oils proved to be superior in the breakdown test.

The cooling capacity of the natural ester worsens with aging. The undesirable, strong increase in the viscosity of natural oils in the course of aging in air leads to technical problems as a coolant medium in transformers.^[3] Therefore, air should be excluded when vegetable oils are used as transformer liquids.

4. Conclusion

In fact, the sustainable substitutes of mineral oils are the biodegradable, low-sulfur, and nontoxic, synthetic, and natural esters of the fatty acids. Concerning the electrical breakdown behavior, the biodegradable fluid has the highest withstand capability compared with the others. However, the high voltage tests cause additional conjugated C=C bonds in the fatty acid chains. The increased peroxide number indicates oxidation and formation of radicals, whereas the content of antioxidants (such as BHT) drops.

Vegetable oils with unsaturated fatty acids are less suitable for unsealed power transformers that have unrestricted access to moisture and air. Crude natural oils pose further challenges with respect to price, storage and handling, homogeneity and availability, oxidation stability, humidity, viscosity, and freezing at cold weather. In particular, the water problem could open up opportunities for future synthetic or chemically modified natural ester oils (e.g.,^[27]).

Acknowledgements

This study was supported by the Bavarian Czech University Agency (BTHA).

Open access funding enabled and organized by Projekt DEAL.

Conflict of Interest

The authors declare no conflict of interest.

Data Availability Statement

Data are available from the authors on reasonable request.

Keywords

breakdown voltage, decomposition products, ecotoxicity, power transformer oils, vegetable oils

Received: March 15, 2021

Revised: April 24, 2021

Published online:

-
- [1] C. Perrier, A. Beroual, *IEEE Electr. Insul. Mag.* **2009**, 25, 6.
- [2] Z. Shen, F. Wang, Z. Wang, J. Li, *Renewable Sustainable Energy Rev.* **2021**, 141, 110783.
- [3] S. Tenbohlen, M. Koch, *IEEE Trans. Power Delivery* **2010**, 25, 825.
- [4] J. I. Jeong, J. S. An, C. S. Huh, *IEEE Trans. Dielectr. Electr. Insul.* **2012**, 19, 156.
- [5] H. Borsi, E. Gockenbach, in Proc. IEEE Int. Conf. Dielectric Liquids, IEEE, Piscataway, NJ **2005**, pp. 377–380.
- [6] T. V. Oommen, *IEEE Electr. Insul. Mag.* **2002**, 18, 6.
- [7] M. Rafiq, Y. Z. Lv, Y. Zhou, K. B. Ma, W. Wang, C. R. Li, Q. Wang, *Renewable Sustainable Energy Rev.* **2015**, 52, 308.
- [8] M. Karthik, N. Narmadhai, *Mater. Today: Proc.* **2020**, <https://doi.org/10.1016/j.matpr.2020.09.482>.
- [9] R. Liao, S. Liang, C. Sun, L. Yang, H. Sun, *Euro. Trans. Electr. Power* **2010**, 20, 518.
- [10] (a) IEC Standard 60156:1995, *Insulating Liquids, Determination of the Breakdown Voltage at Power Frequency, Test Method*, 2nd ed., IEC, Geneva **1995**; (b) M. Baur, L. Calcara, M. Pompili, *IEEE TDEI* **2015**, 22, 2401.
- [11] IEC Standard 60270:2000, *High-Voltage Test Techniques, Partial Discharge Measurements*, 3rd ed., IEC, Geneva **2000**.
- [12] H. Borsi, *IEEE Trans. Electr. Insul.* **1991**, 26, 755.
- [13] *VDI Wärmeatlas*, Springer, Berlin **2013**, p. 162.
- [14] A. Abdelkhalik, H. Elsayed, M. Hassan, M. Nour, A. B. Shehata, M. Helmy, *Egypt. J. Pet.* **2018**, 27, 131.
- [15] R. Matissek, G. Steiner, M. Fischer, *Lebensmittelanalytik*, Springer, Berlin **2014**.
- [16] C. C. Chang, S. W. Wan, *Ind. Eng. Chem.* **1947**, 39, 1543.
- [17] J. W. Alencar, P. B. Alves, A. A. Craveiro, *J. Agric. Food Chem.* **1983**, 31, 1268.
- [18] R. O. Idem, S. P. R. Katikaneni, N. N. Bakhshi, *Energy Fuels* **1996**, 10, 1150.
- [19] K. D. Maher, D. C. Bressler, *Bioresour. Technol.* **2007**, 98, 2351.
- [20] A. W. Schwab, G. J. Dykstra, E. Selke, S. C. Sorenson, E. H. Pryde, *J. Am. Oil Chem. Soc.* **1988**, 65, 1781.
- [21] Z. Wang, I. Cotton, S. Northcote, *IEEE Electr. Insul. Mag.* **2007**, 23, 5.
- [22] P. Kumbhakar, *J. Opt.* **2011**, 40, 33.
- [23] W. Ye, J. Hao, M. Zhu, J. Li, R. Liao, *J. Mol. Liq.* **2020**, 318, 114032.
- [24] W. Liang, Q. Zhipeng, L. Ze, G. Li, *Optik* **2021**, 239, 166873.
- [25] R. Madavan, S. Balaraman, *Eng. Failure Anal.* **2016**, 65, 26.
- [26] R. Villarroel, B. García de Burgos, D. F. García, *Int. J. Electr. Power Energy Syst.* **2021**, 124, 106172.
- [27] K. Wang, F. Wang, J. Li, Z. Huang, Z. Lou, Q. Han, Q. Zhao, K. Hu, *Ind. Crops Prod.* **2019**, 142, 111834.